

Poisson Noise Reduction with Nonlocal-PCA Hybrid Model in Medical X-ray Images

Daniel Kipele¹ and Kenedy A. Greyson^{2,*}

¹ Department of Computer Engineering, Dar es Salaam Institute of Technology, Dar es Salaam, Tanzania;
Email: danielkipele8411@yahoo.com (D.K.)

² Department of Electronics and Telecommunications Engineering, Dar es Salaam Institute of Technology, Dar es Salaam, Tanzania

*Corresponding: kenedyaliila@yahoo.com (K.A.G.)

Abstract—The presence of Poisson noise in medical X-ray images leads to degradation of the image quality. The obscured information is required for accurate diagnosis. During X-ray image acquisition process, weak light results into limited number of available photons, which leads into the Poisson noise commonly known as X-ray noise. Currently, the available X-ray noise removal methods have not yet obtained satisfying total denoising results to remove noise from the medical X-ray images. The available techniques tend to show good performance when the image model corresponds to the algorithm's assumptions used but in general, the denoising algorithms fail to do complete denoise. X-ray image quality could be improved by increasing the X-ray dose value (beyond the maximum medically permissible dose) but the process could be lethal to patients' health since higher X-ray energy may kill cells due to the effects of higher dose values. In this study, the hybrid model that combines the Poisson Principal Component Analysis (Poisson PCA) with the nonlocal (NL) means denoising algorithm is developed to reduce noise in images. This hybrid model for X-ray noise removal and the contrast enhancement improves the quality of X-ray images and can, thus, be used for medical diagnosis. The performance of the proposed hybrid model was observed by using the standard data and was compared with the standard Poisson algorithms.

Keywords—hybrid model, noise reduction, non-local PCA, Poisson PCA, X-ray image

I. INTRODUCTION

X-ray noise is caused by discrete flow of energy particles known as photons [1]. Photons reach the detector element randomly and independent from each other. The counting of photons obeys Poisson distribution [2, 3]. In Poisson distribution, the number of photons y measured by the detector element over a time interval is described by the probability Function (1).

$$P(y | f) = e^{-f} \frac{f^y}{y!}. \quad (1)$$

where f is the expected number of photons measured by the detector element over a time interval and $P(y | f)$ is the standard Poisson distribution.

In X-ray medical imaging, few numbers of photons are collected by the detector element. During acquisition process, weak light source results into limited number of available photons, which leads to Poisson noise known as X-ray noise [4, 5]. The X-ray image quality could be improved by increasing the X-ray dose value (beyond the maximum medically permissible dose) but the process could be lethal to patient health since higher X-ray energy causes cell deaths [6]. So due to the effects of higher X-ray dose values, the digital image denoising techniques is developed to reduce noise in images instead of using increased X-ray dose. Through studies [4, 7–9], the Poisson noise could be handled in two denoising approaches. The first approach involves denoising techniques, which directly investigate the statistical properties of Poisson noise in an image. The second approach involves adaptation of noise from Poisson distribution to Gaussian distribution and then apply normal denoising technique based on Gaussian distributed signal. The denoised image had to be re-converted back to Poisson signal.

The X-ray denoising techniques which directly investigate the statistical properties of X-ray noise in an image, are commonly known as Poisson Direct-denoising methods. The Poisson Direct-denoising methods use dictionary-learning techniques such as Principal Component Analysis (PCA) to learn direct from the noisy image and then separate noise signal from the original image signal. Studies [2, 8, 10] suggest that Poisson direct-denoising methods are relevant when the image suffers from high noise level, which is due to poor resolution of photon counts observation. When the number of photon-counts is large, i.e., when there is good resolution of photon counts observation, the Poisson distribution approaches Gaussian distribution. Jin *et al.* [1] further explain that in large photon-counts observation, the Poisson noise cannot be distinguished from Gaussian noise. Thus, the approach to improve Signal to Noise Ratio (SNR) in large-photon count observation is to reduce the dependence of the noise on the signal by

applying an image transformation. The Anscombe transform is a relied Variance Stabilizing Transform (VST) for stabilizing the variance of the Poisson noise [11–13]. When a VST is applied to a Poisson noise image (z), it treats the Poisson noise image as if the image is corrupted by the noise, which is in Gaussian distribution. Mathematically, the variance stabilization with Anscombe transform $a(z)$ is given in Eq. (2).

$$a(z) = z_{AT} = 2\sqrt{z + \frac{3}{8}}, \quad z = (z_1, \dots, z_N). \quad (2)$$

where N is the pixel numbers.

Thus, by applying Eq. (2) to a Poisson distributed image, it gives a signal whose noise is asymptotically Gaussian distributed and then, denoising $a(z)$ produces the signal which is also in Gaussian distribution. Therefore, an inverse transformation should be applied in order to obtain back the required signal of the interest, which is in Poisson distribution $a^{-1}(z)$. Mathematically, an inverse-VST Anscombe transformation is given in Eq. (3).

$$a^{-1}(z) = \left(\frac{z}{2}\right)^2 - \frac{3}{8}. \quad (3)$$

The X-ray noise removal methods which relay on VST denoising approach are commonly referred to as the Poisson VST-denoising methods. It is explained that, Poisson VST-denoising methods are relevant when the image suffers from moderate noise level, i.e., large-photon emission [7–9].

II. LITERATURE SURVEY

There are various techniques researched on nonlocal (NL) X-ray denoising methods. The nonlocal means denoising method, initially proposed in [14] replaces a noisy pixel in an image with a weighted average of similar pixels located in different regions within an image (i.e., nonlocal selected pixels). Mathematically, the implementation of the original nonlocal (NL) means denoising algorithm is as presented in Eq. (4).

$$v(i) = u(i) + n(i). \quad (4)$$

where $v(i)$ is the observed noise, $u(i)$ is the original image pixel and $n(i)$ is the independent distributed Gaussian noise at the pixel i with zero mean and a certain known variance σ_a^2 . The estimated denoised pixel values in the image $\hat{v}(i)$ was derived as the weighted average of all gray values $\omega(i, j)$ within the search region $s(i)$ [15, 16] as presented in Eq. (5).

$$\hat{v}(i) = \sum_{j \in s(i)} \omega(i, j)v(j). \quad (5)$$

where $\omega(i, j)$ is the amount of similarity between patches centred at i and j , $s(i)$ is the search window, and $v(i)$ is the image patch (that is, the square container of pixels).

The use of the NL means denoising method in removing noise in images became a turn-up from the use of the local denoising methods, which were relying only on the local neighborhood pixels to denoise the image [15]. The researches [14, 16, 17] show that the NL means denoising methods perform well compared to the local neighborhood denoising methods in denoising the images with signal-independent additive white Gaussian noises (AWGN). The researches [14, 15] further stress that the local neighborhood denoising methods results into much loss of image details compared to the NL denoising methods. It is shown that due to the enormous amount of weight computations, the original NL means denoising algorithm has a high computational cost [18, 19]. Approach in [18] uses a dictionary where patches with similar photometric are clustered together. The dictionary was built with high-resolution image and organized in terms of indexing. Its entries were used to search for similar patches quickly, and hence improved denoised results. The method performed well in reducing AWGN. When Dauwe *et al.* [19] ignored contributions of dissimilar patches from the reference noise image by setting their corresponding weights to zero, thus computing only contributions from the similar pixels, the results become better visually than those from the original NL means method and the results were obtained in less computation time than the results in [18, 19]. The method performed well in reducing AWGN.

The strength of the X-ray noise in image depends on the image intensity (i.e., X-ray noise is a signal-dependent noise) [4, 8, 20]. The usual denoising methods, which are based on reducing the signal-independent noises such as AWGN became ineffective in reducing the X-ray noise [8, 20]. The principal component analysis (PCA) is a relied dictionary learning technique for data dimensionality reduction. Some methods employed the dictionary learning techniques into the original NL means denoising methods and these methods successfully reduced the signal-dependent noise (the Poisson noise) in the image. The PCA has been applied to extract uncorrelated details (Poisson noisy) from a large set of image details (pixels) [2, 21]. The approach in [21] introduces adaptive local dictionary for contrast restoration in denoised image and introduced a new statistical distance measure for patch comparison. The method succeeded to reduce Gaussian distributed noise (signal-independent noise) as well as the non-Gaussian distributed noise (signal-dependent noise). It is claimed that Photon-limited imaging arises during image acquisition when the number of photons collected by a sensor array is small relative to the number of detector elements [2]. The method combined Poisson-dictionary learning technique (Poisson-PCA) in nonlocal means denoising method. The notable improvement in this method is an adaption of the number of dictionary elements used with respect to the noise level in the image.

The method succeeded to reduce signal-dependent noise in a photon-limited imaging situation [22, 23].

Furthermore, the review in deep learning-based image super-resolution methods including Convolutional Neural Networks (CNN) and Generative Adversarial Networks (GAN) based on internal network structure is presented by Liu *et al.* [24]. A similar study regarding the setting of image-patch size during super-resolution process and their relations with image's scaling factor to find the best patch size for the algorithms, which may produce better output high-resolution images is discussed by Hamdan *et al.* [25].

III. THE PROPOSED HYBRID MODEL

In this study, the hybrid model for X-ray noise removal and contrast enhancement is proposed following its denoising and contrast enhancement as depicted in Fig. 1. Studies have revealed that X-ray noise could be reduced in X-ray images by two denoising approaches. The first approach involves denoising image by VST denoising method. This method involves adapting noise distribution from Poisson distribution to Gaussian distribution and then apply normal denoising techniques based on Gaussian distribution. The denoised image has to be re-converted back to Poisson signal. As described in section 1, the Poisson VST-denoising approaches are relevant to images which suffer from moderate low noise level i.e., large-photon count images [7–9, 13].

The VST denoising method is performed step by step as described in [13].

Step 1: Apply the Anscombe transformation shown in (2) into Poisson noisy image to obtain asymptotically additive Gaussian noisy image, $a(z)$.

Step 2: Apply a conventional filter (φ) to remove the AWGN as shown by the Eq. (6).

$$\varphi\{a(z)\} = \varphi(z_{AT}) = E\{z_{AT} / z\} \quad . \quad (6)$$

Step 3: Return the denoised image to the original range of z , and then, compute the optimal inverse Anscombe transformation by using Eq. (7).

$$I_a^p : E[a(z) | y] \rightarrow E[z | y] = y \quad . \quad (7)$$

Step 4: Repeat the steps from step 1 until the satisfactory results are obtained.

In Poisson Direct-denoising methods, the statistical properties of X-ray noise in an image are directly investigated. The PCA technique is used to learn the noisy image and separate noise signal from the original image signal.

As described Section I, the Poisson Direct-denoising methods are relevant in images which suffer from high noise i.e., low-photon count images [2, 8, 10]. Mohammed *et al.*, Gonzalez *et al.* [22, 26] claim that the produced medical X-ray images are poorly illuminated and have low contrast.

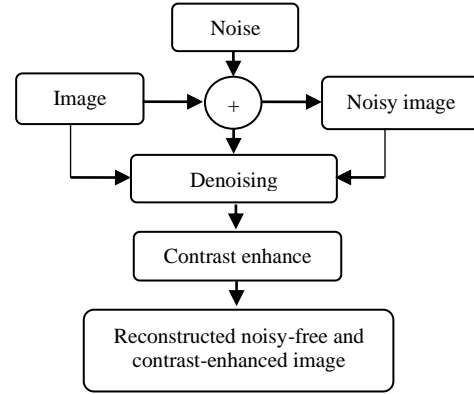


Figure 1. Block diagram of image denoising and contrast enhancement.

This study proposes the development of a hybrid model, which combines the two Poisson denoising approaches in order to have a Poisson denoising method which can perform well on images that suffer from both moderate low and high noise level. It is also stated that the digital contrast enhancement techniques improve quality of image and give support to human visual perception [27]. To have improved quality X-ray images, the proposed hybrid model in this study has been formed by combining the optimal hybrid denoising filter (involving the Poisson Direct-denoising methods and the Poisson VST denoising methods) and the best hybrid enhancement which was formed through hybridizing the competitive digital enhancement methods.

The Signal to Noise Ratio (SNR) in image is given as the ratio of power of a signal to power of background noise. The SNR concept gives a common way of describing the noise power in an image since the noise power is described by considering the maximal noise level in an image. The maximal noise level in image is commonly noted by the term peak value. Thus, by considering the SNR concept, the strong noise in an image is denoted by low peak value (due to high value of denominator, noise) and the weak noise in an image is denoted by high peak value (due to low value of denominator, noise). Studies [2, 7] highlight that Poisson peak values not greater than 4 provide a good evaluation on evaluating the denoising performance of a particular denoising method. In this study, Poisson noisy of peak value 4 has been set as the optimal Poisson noise level in evaluating the denoising performance of the discussed X-ray noise removal methods.

First, in designing the hybrid X-ray noise removal filter shown in Fig. 2, several orders of combinations involving the Poisson-VST denoising technique and Poisson-Direct denoising technique were performed. The combinations performed include serial hybrid of Poisson NL PCA-Direct filter and Poisson NL PCA-VST filter, serial hybrid of Poisson NL PCA-VST filter and Poisson NL PCA-Direct filter, two-step NL PCA-Direct filter and the two-step NL PCA-VST filter.

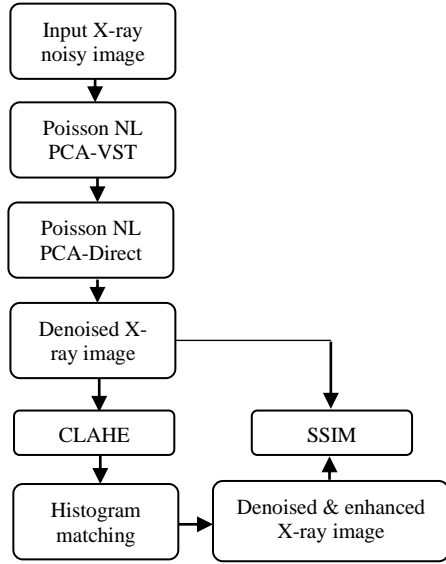


Figure 2. Block diagram of the proposed hybrid model for noise removal and contrast enhancement.

Through the experiments done, the optimal hybrid X-ray noise removal filter obtained was due to a serial denoising order of the Poisson NL PCA-VST filter followed by the Poisson NL PCA-Direct filter.

Second, in designing an optimal hybrid-contrast enhancement method, the contrast enhancement techniques for digital images were applied. The techniques applied included Contrast Limited Adaptive Histogram Equalization (CLAHE), histogram matching, histogram stretching, histogram equalization and unsharp mask techniques. The enhancement performance of the techniques was measured through the image quality assessment technique and by assessing the visual appearance of the enhanced images. The findings show that CLAHE and histogram matching technique resulted into competitive results compared to the results obtained from the other techniques. Lee *et al.* [28] also identified CLAHE as a good technique for enhancing the visibility of local details in an image and the technique has demonstrated success in enhancing low contrast medical images. Due to competitiveness of the CLAHE and histogram matching techniques as compared to other enhancement techniques, the hybrid contrast enhancement method was designed based on the two techniques. The tested enhancement hybrid orders involving the two methods include serial of CLAHE and histogram matching, serial of histogram matching and CLAHE, two-step CLAHE hybrid, two-step CLAHE and histogram matching, two step histogram matching and the two-step histogram matching and CLAHE. The hybrid contrast enhancement method, which resulted into the best result was due to the serial hybridization of CLAHE and histogram matching methods.

Last, the proposed hybrid model for noise removal and contrast enhancement was formed through the integration of hybrid X-ray noise removal filter and hybrid contrast enhancement method.

IV. EXPERIMENTAL RESULTS

The structural similarity index measure (SSIM) is the image-quality measurement technique that compares the structural match between test image and reference image. It is stated in [29] that human eye (human visual system-HVS) is very sensitive to image structural changes, thus an image quality measurement technique which measures structural information change between the test image and the reference image is expected to provide a good approximation to perceived image distortion. Simulations were performed by using MATLAB®.

In this work, non-medical images in Fig. 3 show the efficiency of the proposed method. Discussions show that the SSIM is the best technique to evaluate visual image quality since SSIM output values correlates well with the way human eye perceive visual image quality [30, 31]. The SSIM has a maximum value of one (1). Maximum value is only possible when the test image is completely like the reference image. Values closer to one indicate large similarity between test image and reference image. In this study, the SSIM was used to measure the visual quality of the test image in comparison with the reference image.

Fig. 3(a)–(c) show the results of synthesizing Poisson noise of peak value 4 into the acquired X-ray image [2], and [7]. The generated Poisson noisy corrupted images were used as input data in evaluating the denoising performance of the discussed X-ray noise removal methods (Poisson NL PCA-Direct method, Poisson NL PCA-VST method and the proposed hybrid model for noise removal and contrast enhancement method).

On denoising moderate intensity X-ray images, the X-ray noise removal methods were compared on the denoising the moderate intensity X-ray images. The results show that the denoised images from the proposed hybrid model, (as presented in Fig. 3(j–l), have clearly seen details with high values on the SSIM results compared to the results from the Poisson NL PCA-Direct method as presented in Fig. 3(d–f) and the results from the Poisson NL PCA-VST method as presented in Fig. 3(g–i). From these findings, the study observes that the proposed hybrid model performs well in reducing X ray noise on images with moderate intensity compared to the other discussed Poisson noise removal methods. Secondly, on denoising the lower intensity X-ray images, the X-ray noise removal methods were compared on denoising the X-ray images with lower intensities (X-ray chest Fig. 4(a) and X-ray womb Fig. 4(b)).

There was observed challenge in denoising lower intensity on denoising the lower intensity X-ray images. The challenge was that the visual appearances of the denoised images presented in Fig. 4(c–h) from the X-ray noise removal methods were not impressive for visual presentation, but the SSIM image assessment technique reported numerical results with high numerical values. Thus, this study supports the claim that the SSIM exhibit input dependent behavior in measuring signal distortions [14, 15, 24, 25, 32].

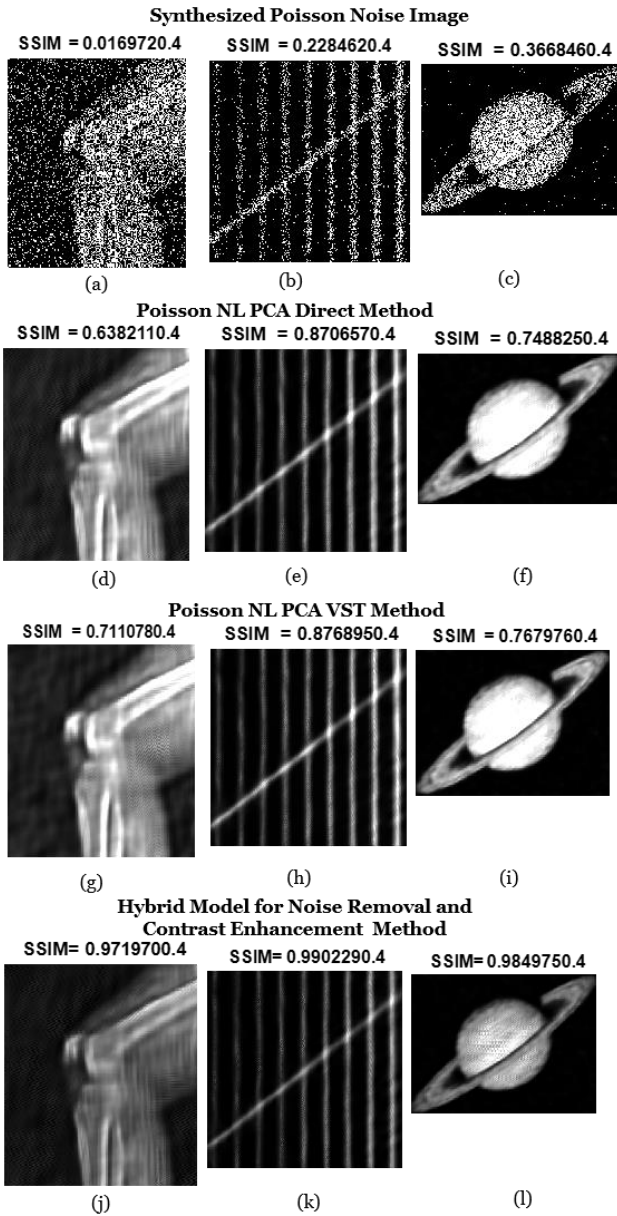


Figure 3. Synthesized Poisson noise images and the denoised images.

According to researches [23, 33], clinical diagnosis with Superior Labral Anteroposterior (SLAP) are challenging. In fact, the physical examination is typically nonspecific. Therefore, proper diagnostic imaging is essential for the diagnosis. Performance of the model by using equivalent SLAP is as shown in Fig. 5.

The researches [22, 26] had also reported that the low intensity medical X-ray images have strong contamination of Poisson noise. Niknejad *et al.* [9] further stressed that lower intensity in images yields stronger noise since the Signal to Noise Ratio (SNR) is obtained by the ratio of relevant details with respect to irrelevant details in an image. Thus, from the SNR concept, it can be deduced that the poor denoising effect in the lower intensity images was due to the large ratio of irrelevant details (strong Poisson noise) present in the image. The denoising performance of the proposed hybrid model with respect to other existing Poisson

denoising methods was also compared to by using the standard Poisson images. The standard Poisson images was used in this study to have standard data, which are common in most Poisson denoising methods as observed in literature. The researchers who had also used the standard Poisson images (Saturn image and Ridges image) include [2, 7].

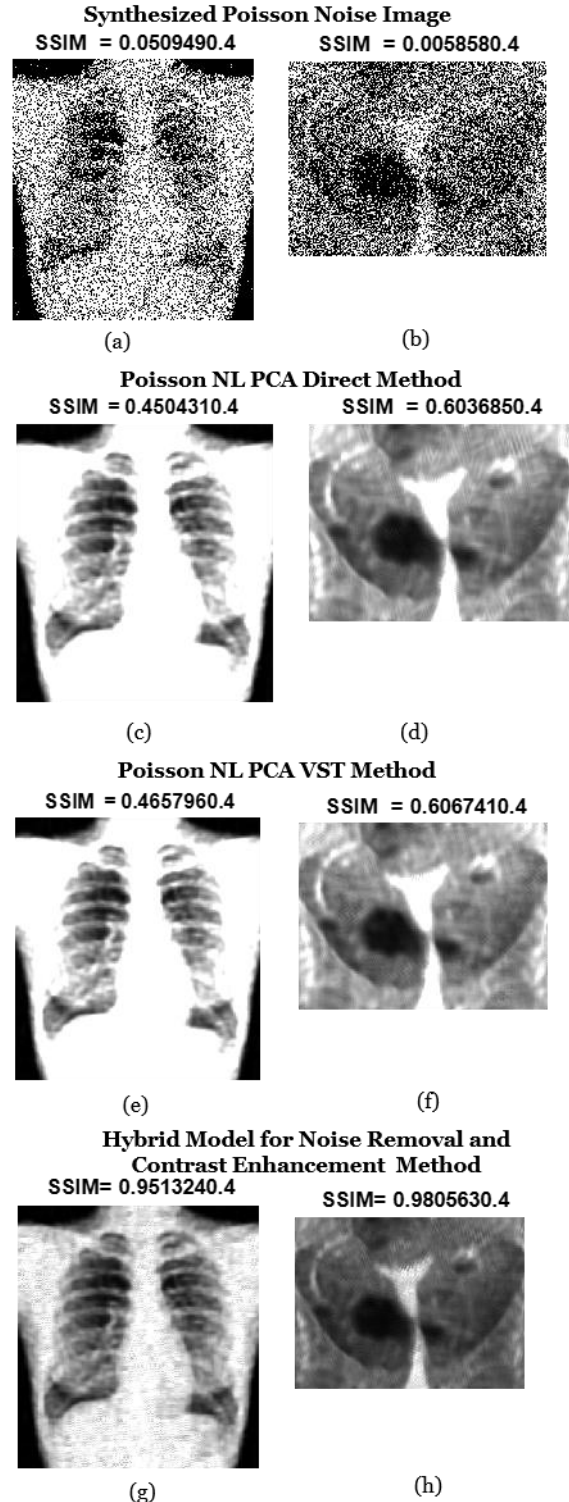


Figure 4. Lower intensity images and the denoised images.

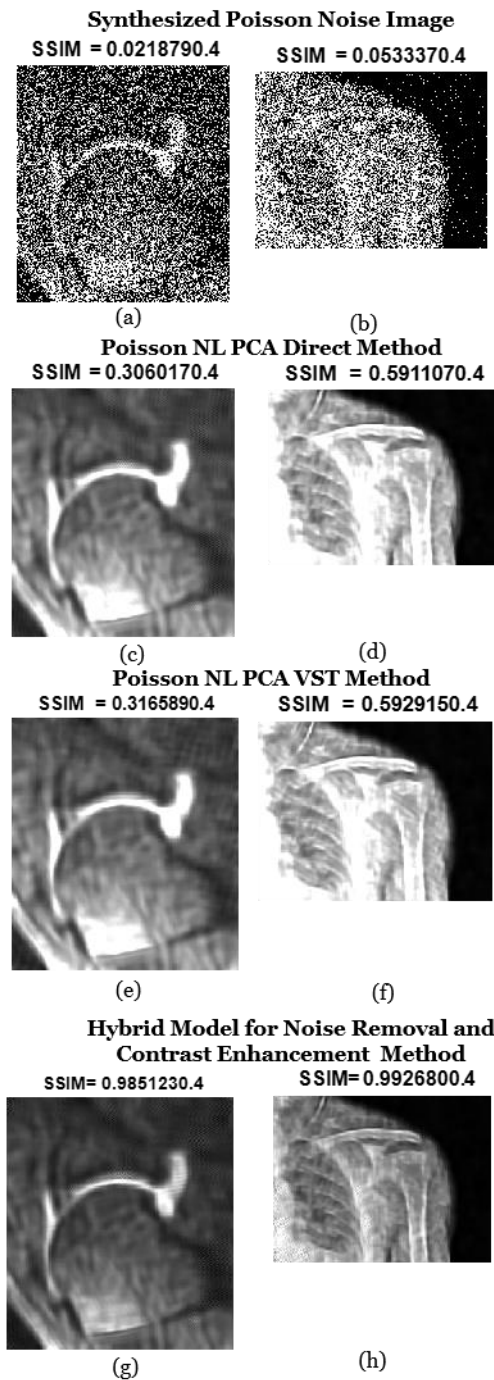


Figure 5. Synthesized Poisson noise image and denoised SLAP tear injuries images using hybrid method.

V. CONCLUSION

The denoising on X-ray images is still a challenge in medical image processing, especially, on the photon-limited images. The proposed hybrid model performed well in reducing the X-ray noise in X-ray images with high intensities as well as in X-ray images with low intensities compared to the other discussed X-ray noise removal methods. Future work is required to assess the measurement accuracy of the SSIM in measuring the X-ray images with lower intensities.

CONFLICT OF INTEREST

The authors declare no conflict of interest.

AUTHOR CONTRIBUTIONS

Kipele made substantial contributions to conception of the presented idea, developed the model and acquisition of data used in the manuscript. Both authors performed the simulation, discussed the results, wrote the manuscript, and approved the final version to be published.

FUNDING

Authors conducted the research and wrote the manuscript with support from Dar es Salaam Institute of Technology (DIT) Research and Publication Unit.

REFERENCES

- [1] Q. Jin, O. Miyashita, F. Tama, J. Yang, and S. Jonic, "Poisson image denoising by piecewise principal component analysis and its application in single-particle X-ray diffraction imaging," *IET Image Processing*, vol. 12, no. 12, pp. 2264–2274, 2018.
- [2] J. Salmon, Z. Harmany, C. Deledalle, and R. Willett, "Poisson noise reduction with Non-local PCA," *Journal of Math Imaging*, vol. 48, pp. 279–294, 2014.
- [3] P. Raj and T. Venkateswarlu, "Denoising of magnetic resonance and X-ray images using variance stabilization and patch-based algorithms," *The International Journal of Multimedia and Its Applications (IJMA)*, vol. 4, no. 6, pp. 53–71, 2012.
- [4] T. V. Kirti, D. H. Omkar, and S. M. Ashok, "Poisson noise reducing bilateral filter," *Procedia Computer Science*, vol. 79, pp. 861–865, 2016.
- [5] Y. Sun, X. Liu, P. Cong, L. Li, and Z. Zhaoa, "Digital radiography image denoising using a generative adversarial network," *Journal of X-ray Science and Technology*, vol. 26, no. 4, pp. 523–534, 2018.
- [6] T. Kirti, K. Jitendra, and S. Ashok, "Poisson noise reduction from X-ray images by region classification and response median filtering," *Indian Academy of Sciences, Sādhanā*, vol. 42, no. 6, pp. 855–863, 2017.
- [7] R. Giryes, and M. Elad, "Sparsity Based Poisson Denoising with dictionary learning," *IEEE Transactions of Image Process*, vol. 23, no. 12, pp. 5057–5069, 2014.
- [8] W. Feng, H. Qiao, and Y. Chen, "Poisson noise reduction with higher-order natural image prior model," *SIAM Journal on Imaging Sciences*, vol. 9, no. 3, pp. 1502–1524, 2016.
- [9] M. Niknejad, and M. A. T. Figueiredo, "Poisson image denoising using best linear prediction: A post-processing framework," in *Proc. Conference 26th European Signal Processing (EUSIPCO)*, Rome, Italy, 2018.
- [10] C. Deledalle, J. Salmon, and A. Dalalyan, "Image denoising with patch based PCA: Local versus global," in *Proc. 22nd British Machine Vision Conference*, Dundee, UK, 2011, pp. 1–10.
- [11] F. J. Anscombe, "The transformation of Poisson, binomial and negative-binomial data," *Biometrika*, vol. 35, pp. 246–254, 1948.
- [12] D. N. H. Thanh, V. B. S. Prasath, and L. M. Hieu, "A review on CT and X-ray images denoising methods," *Informatica*, vol. 43, no. 2, pp. 151–159, 2019.
- [13] S. S. Ahmed, Z. Messali, F. Poyer, L. L. L. Rouic, L. Desjardins, N. Cassoux, C. D. Thomas, S. Marco, and S. Lemaitre, "Iterative variance stabilizing transformation denoising of spectral domain optical coherence tomography images applied to retinoblastoma," *Ophthalmic Research*, vol. 59, no. 3, pp. 164–169, 2018.
- [14] A. Buades, B. Coll, and J. M. Morel, "A non-local algorithm for image denoising," in *Proc. IEEE International Conference on Computer Vision and Pattern Recognition*, San Diego, CA, USA, 2005, pp. 20–25.
- [15] F. Dacke, "Non-local means denoising of projection images in cone beam computed tomography," M.S. thesis, School of

- Engineering Sciences, Dept. Mathematical Statistics, Royal Institute of Technology Stockholm, 2013.
- [16] T. Tasdizen, "Principal neighborhood dictionaries for non-local means image denoising," *IEEE Trans Image Process*, vol. 18, no. 12, pp. 2649–2660, 2009.
 - [17] T. Brox, O. Kleinschmidt, and D. Cremers, "Efficient nonlocal means for denoising of textural patterns," *IEEE Transactions on Image Processing*, vol. 17, no. 7, pp. 1083–1092, 2008.
 - [18] H. Bhujle and S. Chaudhuri, "Novel speed-up strategies for non-local means denoising with patch and edge patch-based dictionaries," *IEEE Transactions on Image Processing*, vol. 23, no. 1, pp. 356–365, 2014.
 - [19] A. Dauwe, B. Goossens, H. Luong, and W. Philips, "A fast non-local image denoising algorithm," in *Proc. International Society for Optical Engineering*, vol. 6812, 2008.
 - [20] S. S. Raj, "Foveated Non-Local means denoising for color images, with cross-channel paradigm," M.S. thesis, Tampere University of Technology, 2016.
 - [21] C. Kervrann, J. Boulanger, and P. Coupé, "Bayesian Non-local means filter, image redundancy and adaptive dictionaries for noise removal," *Scale Space and Variational Methods in Computer Vision*, vol. 4485, pp. 520–532, 2007.
 - [22] F. G. Mohammed, H. M. Rada, and S. G. Mohammed, "Contrast and brightness enhancement for low medical X-ray images," *International Journal of Scientific and Engineering Research*, vol. 4, no. 5, pp. 1519–1523, 2013.
 - [23] J. Grubin, A. Maderazo, and D. Fitzpatrick, "Imaging evaluation of superior labral anteroposterior (SLAP) tears," *The American Journal of Orthopedics*, vol. 44, no. 10, pp. 476–477, 2015.
 - [24] Y. Liu, Y. Qiao, Y. Hao, and F. Wang, "Single image super resolution techniques based on deep learning: status, applications and future directions," *Journal of Image and Graphics*, vol. 9 no. 3, pp. 74–86, 2021.
 - [25] S. Hamdan, Y. Fukumizu, T. Izumi, and H. Yamauchi, "Face image super-resolution with adaptive patch size to scaling factor," *Journal of Image and Graphics*, vol. 6, no. 2, pp. 167–173, 2018.
 - [26] R. C. Gonzalez and R. E. Woods, *Digital Image Processing*, 3rd ed. Upper Saddle River, New Jersey Pearson Education, Inc. 2008.
 - [27] I. A. Humied and F. E. A. Chadi, "Image contrast enhancement techniques: A comparative study of performance," *International Journal of Computer Applications*, vol. 137, no. 13, pp. 43–48, 2016.
 - [28] J. Lee, S. R. Pant, and H. S. Lee, "An adaptive histogram equalization based local technique for contrast preserving image enhancement," *International Journal of Fuzzy Logic and Intelligent Systems*, vol. 15, no. 1, pp. 35–44, 2015.
 - [29] M. Gogoi and M. Ahmed, "Image quality parameter detection: A study," *International Journal of Computer Sciences and Engineering*, vol. 4, no. 7, pp. 110–116, 2016.
 - [30] J. F. Pambrun and R. Noumeir, "Limitations of the SSIM quality metric in the context of diagnostic imaging," in *Proc. International Conference on Image Processing (ICIP)*, Quebec City, QC, Canada, pp. 2960–2963, 2015.
 - [31] C. S. Varnan, A. Jagan, J. Kaur, D. Jyoti, and D. S. Rao, "Image quality assessment techniques PN spatial domain," *International Journal of Computer Science and Technology*, vol. 2, no. 3, pp. 177–184, 2011.
 - [32] J. Malo, R. Navarro, I. Epifanio, F. Ferri, and J. M. Artigas, "Non-linear invertible representation for joint statistical and perceptual feature decorrelation," in *Proc. the Joint IAPR International Workshops on Advances in Pattern Recognition*, Berlin, pp. 658–667, 2020.
 - [33] D. A. Lansdown, I. Bendich, D. Motamedi, and B. T. Feeley, "Imaging-based prevalence of superior labral anterior-posterior tears significantly increases in the aging shoulder," *Orthopaedic Journal of Sports Medicine*, vol. 6, no. 9, 2018.

Copyright © 2023 by the authors. This is an open access article distributed under the Creative Commons Attribution License ([CC BY-NC-ND 4.0](https://creativecommons.org/licenses/by-nc-nd/4.0/)), which permits use, distribution and reproduction in any medium, provided that the article is properly cited, the use is non-commercial and no modifications or adaptations are made.